Atmos. Meas. Tech. Discuss., 7, 3471–3501, 2014
www.atmos-meas-tech-discuss.net/7/3471/2014/
doi:10.5194/amtd-7-3471-2014
© Author(s) 2014. CC Attribution 3.0 License.

Atmospheric Measurement Techniques Discussions

This discussion paper is/has been under review for the journal Atmospheric Measurement Techniques (AMT). Please refer to the corresponding final paper in AMT if available.

Derivation of tropospheric methane from TCCON CH_4 and HF total column observations

K. M. Saad[1], D. Wunch[1], G. C. Toon[1,2], P. Bernath[3], C. Boone[4], B. Connor[5], N. M. Deutscher[6,7], D. W. T. Griffith[6], R. Kivi[8], J. Notholt[7], C. Roehl[1], M. Schneider[9], V. Sherlock[10], and P. O. Wennberg[1]

[1]California Institute of Technology, Pasadena, CA, USA
[2]Jet Propulsion Laboratory, California Institute of Technology, Pasadena, CA, USA
[3]Old Dominion University, Norfolk, VA, USA
[4]University of Waterloo, Waterloo, Ontario, Canada
[5]BC Consulting, Ltd., Alexandra, New Zealand
[6]University of Wollongong, Wollongong, Australia
[7]University of Bremen, Bremen, Germany
[8]Finnish Meteorological Institute, Sodankylä, Finland
[9]Karlsruhe Institute of Technology, Karlsruhe, Germany
[10]National Institute of Water and Atmospheric Research, Wellington, New Zealand

Received: 15 February 2014 – Accepted: 11 March 2014 – Published: 7 April 2014

Correspondence to: K. M. Saad (katsaad@caltech.edu)

Published by Copernicus Publications on behalf of the European Geosciences Union.

Abstract

The Total Carbon Column Observing Network (TCCON) is a global ground-based network of Fourier transform spectrometers that produce precise measurements of column-averaged dry-air mole fractions of atmospheric methane (CH_4). Temporal variability in the total column of CH_4 due to stratospheric dynamics obscures fluctuations and trends driven by tropospheric transport and local sources and sinks. We remove the contribution of stratospheric variability from the total column average by subtracting an estimate of the stratospheric CH_4 derived from simultaneous measurements of hydrogen fluoride (HF). HF provides a proxy for stratospheric CH_4 because it resides solely in the stratosphere, has a nearly linear inverse relationship with stratospheric CH_4, and is measured at most TCCON stations. The stratospheric partial column of CH_4 is calculated as a function of the zonal and annual trends in the relationship between CH_4 and HF in the stratosphere, which we determine from ACE-FTS satellite data. We also explicitly take into account the CH_4 column averaging kernel to estimate the contribution of stratospheric CH_4 to the total column. The resulting tropospheric CH_4 columns are consistent with in situ aircraft measurements and augment existing observations in the troposphere.

1 Introduction

The most abundant hydrocarbon in the atmosphere, methane (CH_4) is a driver of background tropospheric chemistry and a significant radiative forcing gas. However, the long-term trends of atmospheric mixing ratios and fluctuations in the annual growth rate remain unexplained due to an incomplete understanding of its sources and sinks.

Analyses of temporal and geospatial trends of CH_4 thus require precise, continuous measurements with adequate spatial coverage. Several such monitoring networks, such as WMO Global Atmospheric Watch and National Oceanic and Atmospheric Administration (NOAA) Global Monitoring Division, have measured methane for decades.

AMTD
7, 3471–3501, 2014

These sites are often in locations primarily intended for background observations, and measurements are confined to the surface, primarily within the boundary layer. The Total Carbon Column Observing Network (TCCON), a ground-based network of Fourier transform spectrometers (FTS), measures dry-air mole fractions (DMFs) of several atmospheric trace gases, including CH_4, integrated over the entire atmospheric column. The column measurements are sensitive to the free troposphere in addition to the surface, which can allow for better separation of transport vs. local emissions. Additionally, total column measurements are less sensitive to vertical transport and mixing, and thus meridional or zonal gradients in column measurements characterize regional-scale fluxes more closely than surface observations (Yang et al., 2007; Wunch et al., 2011a; Keppel-Aleks et al., 2011).

Nonetheless, tropospheric trends of CH_4 are obscured in total column measurements by variability originating in the stratosphere, especially by vertical shifts of the tropopause. Several methods for accounting for stratospheric variability have been proposed, including incorporating the compact relationship between CH_4 and another chemical tracer in the stratosphere (e.g., Washenfelder et al., 2003; Payne et al., 2009; Angelbratt et al., 2011; Sepúlveda et al., 2012, 2014). Washenfelder et al. (2003) estimated the contribution of variations in stratospheric CH_4 as the product of the hydrogen fluoride (HF) column-averaged DMF, retrieved from the Kitt Peak National Solar Observatory FTS, and the CH_4–HF relationship, calculated from Halogen Occultation Experiment (HALOE) satellite and the JPL MkIV Interferometer data. Wang et al. (2014) similarly use the stratospheric N_2O–CH_4 relationship and the fact that tropospheric N_2O is well known and quiescent to infer stratospheric variations in N_2O, and hence CH_4. Angelbratt et al. (2011) remove NDACC CH_4 total column variability with a multiple regression model that parameterizes anomalies of several measurements, including HF, carbon monoxide (CO), ethane (C_2H_6), and tropopause height. Sepúlveda et al. (2012) use the retrieval algorithm PROFFIT to infer vertical CH_4 profiles directly from the absorption line shapes of the mid-infrared (MIR) FTS spectra measured within the Network for the Detection of Atmospheric Composition Change (NDACC), comparing

AMTD
7, 3471–3501, 2014

the resulting tropospheric columns with those calculated with a HF proxy method. Vertical profile retrievals using the TCCON spectra are more difficult than using NDACC MIR spectra because the NDACC measurements use spectral filters to narrow the spectral coverage, yielding higher signal-to-noise ratios at higher spectral resolution, at the expense of making simultaneous measurements of some other gases. In addition, in general the line strengths in the MIR are higher and doppler widths are smaller, allowing more degrees of freedom in the vertical retrieval. Nevertheless, these retrievals are sensitive to error in the instrument and assumed spectroscopic lineshapes. Quantifying the variability of stratospheric CH_4 via a chemical tracer is, however, not without challenge, as this method is sensitive to error in the representation of the relationship between that tracer and CH_4 in the stratosphere and knowledge of their respective averaging kernels. In addition, this method provides no information about vertical structure within the troposphere.

To determine the stratospheric CH_4 component of the FTS-retrieved total column, we propose to use its relationship to HF, which is measured at almost all TCCON sites. Stratospheric CH_4 has a nearly linear inverse relationship with HF, which has no tropospheric sources (Luo et al., 1995; Washenfelder et al., 2003). The photodissociation of chlorofluorocarbons (CFCs) and the resulting carbonyl products produces free fluorine, which can then in turn react with CH_4 and H_2O to produce HF, the most stable reservoir species of fluorine in the stratosphere (Luo et al., 1994). The reactions producing HF occur in the middle-high stratosphere, leading to a uniformly increasing vertical profile (Luo et al., 1995). CH_4, by contrast, is transported from the troposphere and is destroyed by hydroxyl, chlorine and fluorine free radical-initiated oxidation. The resulting nearly linear relationship between HF and stratospheric CH_4, which is seasonally and zonally consistent, makes HF a reliable proxy for the contribution of stratospheric variability to the CH_4 total column.

AMTD
7, 3471–3501, 2014

2 Derivation of tropospheric CH_4 columns

TCCON FTS retrievals are conducted with the GFIT nonlinear least-squares fitting algorithm, which determines a vertical scale factor (γ) of an a priori vertical profile ($\boldsymbol{x}^{a}$) based on the best spectral fit of the solar absorption signal. The scaled profile is then vertically integrated, and the resulting column abundance is divided by the vertical column of dry air, calculated using the retrieved column of oxygen (O_2) (Wunch et al., 2010, 2011a). Several TCCON stations are near in situ sites that provide surface, tall tower, and aircraft measurements, which we use to compare the final tropospheric column-average CH_4 DMFs.

The linear relationship between CH_4 and HF in the stratosphere can be described as:

$$\boldsymbol{x}_{CH_4} = c^{trop}_{CH_4}\boldsymbol{u} + \beta \boldsymbol{x}_{HF} \quad (1)$$

where $\boldsymbol{x}$ represents the true profile of each of the respective trace gases, $c^{trop}_{CH_4}$ is the pressure-weighted DMF averaged over the tropospheric column, $\boldsymbol{u}$ is a unity vector the length of the number of vertical levels in the total column retrieval integration, and β is the time-dependent CH_4–HF slope in the stratosphere. Integrating the vertical profiles, the column-averaged form of this relationship becomes:

$$c_{CH_4} = c^{trop}_{CH_4} + \beta c_{HF} \quad (2)$$

where c is the total column DMF of the respective trace gases. The βc_{HF} term estimates the amount by which stratospheric CH_4 reduces the total column, rather than the stratospheric partial column of CH_4.

The retrieved integrated column of CH_4 can be expressed as a first order Taylor expansion about the solution $\gamma_{CH_4} c^{a}_{CH_4}$ (Rodgers and Connor, 2003) such that,

$$\hat{c}_{CH_4} = \gamma_{CH_4} \cdot c^{a}_{CH_4} + \boldsymbol{a}^{\S}_{CH_4}(\boldsymbol{x}_{CH_4} - \gamma_{CH_4}\boldsymbol{x}^{a}_{CH_4}) \quad (3)$$

AMTD
7, 3471–3501, 2014

where $\hat{c}$ is the retrieved column, γ_{CH_4} is the retrieved profile scale factor, and $\boldsymbol{x}^{\mathbf{a}}_{\mathbf{CH_4}}$ and $c^{a}_{CH_4}$ are the a priori vertical profile and column-integrated CH_4, respectively. We define **§** as an operator that represents the pressure-weighted integration of the profile:

$$\boldsymbol{a}^{\S}\boldsymbol{x} = \sum_{i=1}^{N} a_i \cdot h_i \cdot x_i \tag{4}$$

where $\boldsymbol{a}$ the FTS column averaging kernel, dependent on solar zenith angle, $\boldsymbol{h}$ is the pressure weighting function, such that $\hat{c} = \boldsymbol{h}^T \hat{\boldsymbol{x}}$ (Connor et al., 2008; Wunch et al., 2011b), and i is the index of pressure levels from the surface to the highest level, N. When the vertical column includes water vapor, such as in the case of the priors, the pressure weighting function incorporates the H_2O profile to convert $\boldsymbol{x}$ to dry-air mole fractions.

By combining Eqs. (1) and (2) into Eq. (3), we can derive a tropospheric column-average DMF:

$$c^{\text{trop}}_{CH_4} = \hat{c}_{CH_4} - \beta\left(\gamma_{CH_4} \cdot c^{a}_{HF} + \boldsymbol{a}^{\S}_{\mathbf{CH_4}}\left(\boldsymbol{x}_{\mathbf{HF}} - \gamma_{CH_4}\boldsymbol{x}^{\mathbf{a}}_{\mathbf{HF}}\right)\right). \tag{5}$$

Ideally, $\boldsymbol{x}_{\mathbf{HF}}$ would be derived from the equivalent of Eq. (3) for HF, but doing so would require inverting the pressure-weighted averaging kernel, which does not have a unique solution. Thus, in order to solve Eq. (5), we must assume that $\boldsymbol{x}_{\mathbf{HF}} = \hat{\boldsymbol{x}}_{\mathbf{HF}} = \gamma_{HF}\boldsymbol{x}^{\mathbf{a}}_{\mathbf{HF}}$ and, accordingly, that the shape of the HF profile is known. In general, this is a reasonable assumption because the vertical profile is governed mainly by well-characterized chemical production, and, as previously stated, increases uniformly. However, this solution has limitations when the scaled profile deviates from the true profile, such as in the polar vortex.

Substituting $\gamma_{HF}\boldsymbol{x}^{\mathbf{a}}_{\mathbf{HF}}$ for $\boldsymbol{x}_{\mathbf{HF}}$, the tropospheric column of CH_4 is derived as:

$$c^{\text{trop}}_{CH_4} = \hat{c}_{CH_4} - \beta\left(\gamma_{CH_4} \cdot c^{a}_{HF} + \boldsymbol{a}^{\S}_{\mathbf{CH_4}}\boldsymbol{x}^{\mathbf{a}}_{\mathbf{HF}}\left(\gamma_{HF} - \gamma_{CH_4}\right)\right). \tag{6}$$

AMTD
7, 3471–3501, 2014

All of the terms on the right hand of the equation can be generated from the TCCON dataset except for β, which we derive from ACE-FTS data.

The $c^{\text{trop}}_{\text{CH}_4}$ error is calculated by propagating the uncertainties of the retrievals, which in Eq. (6) are associated with the vertical scale factors, and β, which is described in Sect. 2.1. These errors were propagated as the sum of the squares of the standard errors for each term. For this analysis, we include only those measurements with final errors of less than 1 %.

2.1 Determination of CH_4–HF slope

Vertical profiles of CH_4 and HF mole fractions were developed from level 2, version 3.0 and 3.5 retrievals from the Atmospheric Chemistry Experiment Fourier Transform Spectrometer (ACE-FTS) instrument on the Canadian SCISAT-1 satellite. SCISAT-1 orbits in low Earth orbit with an inclination of 74°, offering coverage of tropical, mid-latitude and polar regions from 85° N to 85° S (Bernath, 2005). Data were taken from February 2004 through December 2012 and filtered to exclude physically unlikely occultations and all CH_4 and HF mole fractions with errors above 5 %. Because HF is not produced in the troposphere, any coincident retrievals of CH_4 and HF were assumed to reside in the stratosphere; therefore we did not designate a pressure level threshold to isolate the stratosphere. Data above 70 km were excluded for consistency with TCCON retrievals, although CH_4 concentrations are generally depleted at that altitude. Annual slopes follow the long-term trend from Washenfelder et al. (2003), given the expected trajectory of HF concentrations in the stratosphere (Fig. 2).

Tracer–tracer relationships in the stratosphere tend to be dependent on latitude, with the tropics exhibiting different slopes than the mid-latitude "surf zone" and the polar regions (Luo et al., 1995). While ACE-FTS coverage of the high latitudes is extensive, tropical coverage is more sparse; thus, to ensure a large enough number of data points in the tropics for robust statistical analysis, we binned CH_4 and HF mole fractions in 30° zonal bands. The tracer relationship demonstrates a clear zonal trend: the slopes

AMTD
7, 3471–3501, 2014

are less steep in lower latitudes, and the Northern Hemisphere slopes are more steep than their zonal counterparts in the Southern Hemisphere (Fig. 1). To determine statistically robust values for β, the CH_4–HF slope was computed for bootstrap subsamples of 1000 individual retrievals from each year and zonal band. In order to minimize the effect of outliers in the determination of the slope, we applied an iteratively-reweighted least squares regression with a Tukey's biweight function, weighting data points by pressure. The mean and 2σ standard deviations of the resulting probability distributions were taken respectively as the values and errors of β (Table 1). For 2013, for which data past March are unavailable, we calculated the annual growth rate of the CH_4–HF ratio in the northern mid-latitude region (30–60° N), chosen because the surf zone is well-mixed and thus has the most robust tracer relationships, and added it to the respective zonal values for 2012. The error for β in 2013 was computed as the sum in quadrature of the error for β in 2012, the standard error of the annual growth rate, and the 2σ standard deviations of the interannual variability of each zonal band. While temporal trends in β do indicate seasonal variability, the impact on the slopes is not sufficiently statistically robust from year to year to incorporate a seasonally-varying β. The sensitivity of the tropospheric methane calculation to β differs by site, but generally varies by 0.1–1 ppb for $\Delta\beta$ of 10.

2.2 Validation of methodology

Equation (6) incorporates two major assumptions: that the CH_4–HF relationship is linear, and that the retrieved HF column is a close approximation to the true HF column. To test these assumptions, we compared tropospheric CH_4 DMFs derived directly from ACE-FTS CH_4 profiles to those calculated by substituting TCCON priors and ACE-FTS CH_4 and HF profiles into Eq. (5). For this analysis, the ACE-FTS trace gas profiles interpolated onto a 1 km vertical grid were considered the true profiles $\boldsymbol{x}_{\mathbf{HF}}$ and $\boldsymbol{x}_{\mathbf{CH_4}}$, and assuming $\gamma_{CH_4} \approx 1$, we solved Eqs. (3) and (5) for $c^{trop}_{CH_4}$. Mole fractions of CH_4 and H_2O below the minimum retrieval altitude were extrapolated using TCCON priors, and

AMTD
7, 3471–3501, 2014

profiles extended up to 70 km. Occultations with CH_4, HF and H_2O errors greater than 10 % were excluded for latitudes poleward of ±30°. In the tropics, the error threshold was relaxed to 40 % in order to ensure a large enough dataset for results to be meaningful. We then compared the calculated tropospheric methane column-averaged DMF to the ACE-FTS CH_4 profiles integrated to the tropopause. For the intercomparison, the integrated ACE-FTS profiles were smoothed with the TCCON CH_4 averaging kernel and priors (Connor et al., 2008; Wunch et al., 2011b). The tropopause altitude was calculated using NCEP Reanalysis local noon temperature profiles, from which the TCCON priors are generated, for consistency.

As Fig. 3 illustrates, the temporal and zonal dependencies of the tropospheric methane calculation are well characterized, with a few notable exceptions. The consistency of the bias across years indicates that the annual variability of β is accurate, although the drift apparent in the northern tropics could be a result of the smaller number of data points that could be included in the determination of β. The underestimation of tropospheric CH_4 in the Northern Hemisphere and slight overestimation in the Southern Hemisphere is a result of the lack of a secular trend in the TCCON a priori HF profiles. The seasonal variability associated with descent within the polar vortices, not currently captured by the HF priors, accounts for the outliers apparent in upper latitudes. Because the southern polar vortex is stronger and more persistent than in the north, the calculated tropospheric column exhibits a much larger spread.

3 Results

Tropospheric column-averaged DMFs were calculated for TCCON sites in Sodankylä (Fig. 4a), Bremen (Fig. 4b), Park Falls (Fig. 4c), Lamont (Fig. 4d), Izaña (Fig. 5a), Darwin (Fig. 5b), Wollongong (Fig. 6a) and Lauder (Fig. 6b). Location information for each of these TCCON sites can be found in Table 2. As we would expect, the tropospheric column-averaged DMFs of CH_4 are higher than the total column DMFs. Many of the low outliers in the total column no longer appear in the tropospheric DMFs. Additionally,

AMTD
7, 3471–3501, 2014

the tropospheric calculation removes most of the effects of the seasonal cycle of stratospheric variability, except in the case of Izaña, which is located on a mountain at about 2.4 km and thus is more sensitive to the free troposphere. While the magnitude of the impact on the seasonal cycle of CH_4 varies from site to site, the tropospheric column calculation generally shifts the peak of CH_4 from late fall to winter and the minimum from spring to late summer. The detrended seasonal cycle at Lamont shows a two-month lag in the maximum and one-lag in the minimum, as well as fewer short-term fluctuations within seasons (Fig. 7). The variances of the tropospheric DMFs over a given day are generally equivalent to those of the corresponding total column DMFs, although the tropospheric standard deviations are in some cases significantly larger than those of the the total column. Sites in the tropics are especially susceptible to both larger errors for a single measurement and larger daily variances due to the higher HF errors caused by H_2O interference (e.g. Darwin, Fig. 5b).

3.1 Comparison to Washenfelder method

The derivation introduced here improves on the previous calculation of Washenfelder et al. (2003) by explicitly including the CH_4 averaging kernels in the estimate of stratospheric loss and including the recent ACE-FTS satellite dataset, that allows for the analysis of temporal and zonal dependencies. To assess the impacts of these additions to the tropospheric CH_4 column, we calculated the tropospheric CH_4 DMFs using the Washenfelder et al. (2003) derivation (Eq. 2) and the annual northern mid-latitude values of β (Table 1, column 6) for all sites. The inclusion of the CH_4 averaging kernel reduces the amplitude of the CH_4 seasonal cycle, which can be attributed to the higher solar zenith angles during winter (Fig. 8). Additionally, the inclusion of the CH_4–HF relationship as a function of latitude allows for more meaningful geospatial comparisons.

AMTD
7, 3471–3501, 2014

3.2 Comparison to in situ measurements

Following the method for numerical integration of in situ profiles derived in Wunch et al. (2010), smoothed column-averaged DMFs were derived from several aircraft campaigns (Table 3). Additional information on the TCCON calibration, including instruments, can be found in Wunch et al. (2010), and the WMO calibration scales used for the instruments can be found in Dlugokencky (2005). Aircraft profiles were integrated to the tropopause, determined using the flight temperature profiles. Aircraft errors are calculated as the sum in quadrature of the respective 2σ instrument errors and the estimated uncertainties associated with the profile not reaching the tropopause and the surface. FTS columns were calculated with the aircraft calibration factors for CH_4 determined in Wunch et al. (2010) applied to the tropospheric column and thus do not include the spectroscopy bias that exists in the total column. FTS errors are calculated as the standard deviation of tropospheric DMFs with individual errors of less than 10 % measured within one hour of each flight. Both the slope and associated error are calculated considering both the aircraft and FTS errors, assuming those errors are independent of each other, following the method outlined in York et al. (2004). Additionally, because the derivation method is predicted to vary linearly, we calculate the slope assuming a y-intercept of zero.

The FTS tropospheric columns show general agreement to each other (Fig. 9), with a slope close to within error of the one-to-one line and a slope and error similar to that of total column CH_4 (Wunch et al., 2010). The tropospheric column calibration curve has a slight hemispheric bias, with Southern Hemisphere sites above the fit line and Northern Hemisphere sites below, with the INTEX campaign, over Park Falls, WI, as the only exception. This trend is consistent with the results of the method validation using the ACE profiles and thus could also be caused by the a priori HF profiles (Fig. 3).

Additionally, we compared the tropospheric CH_4 to long-term in situ flask measurements collected at the Atmospheric Radiation Measurement Program (ARM), Southern Great Plains (SGP) site, near the Lamont TCCON station, and analyzed by the NOAA

AMTD
7, 3471–3501, 2014

Earth System Research Laboratory (ESRL). Surface measurements are collected from a 60 m tower, typically once per week on one afternoon, and aircraft samples are collected approximately weekly with a flight path centered over the tower. The integrated aircraft DMFs are generally higher than the TCCON tropospheric columns, which provide a lower bound to the flask measurements (Fig. 10a). The partial aircraft columns, restricted to the free troposphere (approximately 3–7 km), are more consistent with the TCCON tropospheric columns, indicating that the daily median tropospheric CH_4 column is a good measure of the mixed layer concentration. The calibration curve reinforces this distinction between the aircraft tropospheric and partial tropospheric columns (Fig. 10b); while the best fit slopes, calculated as in (Fig. 9), are equal within measurement error, the slope of the free troposphere partial column has a smaller offset from the FTS-aircraft one-to-one line.

In situ measurements at the surface are also useful for regions without large local surface sources and if the troposphere is well-mixed, as in New Zealand. We compared Lauder FTS measurements to in situ data at the Baring Head National Institute of Water and Atmospheric Research of New Zealand (NIWA) facility, about 600 km northeast of the TCCON site (41.4° S, 174.9° E, 85 m a.s.l.). The Baring Head flask measurements are collected on a stationary platform at a sampling height of 10 m, analyzed with a flame ionizing detector, and calibrated with the NOAA04 scale (Lowe et al., 1991). The surface measurements show strong agreement with the tropospheric columns, both in terms of the DMF values and the amplitude and timing of the seasonal cycle (Fig. 11). The Lauder tropospheric columns are notably higher in the late summer and early fall, which could be a function of local CH_4 sources near Lauder, changing wind directions impacting the covariance between the two sites, or seasonal HF variability not captured in the tropospheric column derivation. Given the relatively large discrepancy of about 10 ppb between the two datasets during those months and the low sensitivity of the tropospheric column to small changes in β, the last of these explanations is the least likely.

AMTD
7, 3471–3501, 2014

4 Conclusions

Inadequate constraints on the global CH_4 budget have been a long-standing problem, and understanding recent trends depends on reliable and frequent observations of tropospheric CH_4 concentrations. By explicitly taking into account the averaging kernels of CH_4 and incorporating temporally and spatially varying estimates of the CH_4–HF relationship, the methodology described here refines earlier tracer proxy methods for estimating stratospheric CH_4. The tropospheric column measurements of CH_4 derived from TCCON total column-averaged DMFs provide a useful addition to existing data sets used to analyze the global methane cycle and verify chemical transport models.

While the CH_4–HF relationship is robust, the calculation of β still has limitations. The slight non-linearity and seasonal variability of the CH_4–HF relationship could impact the estimation of stratospheric CH_4 loss. Further analysis of ACE-FTS and other high-frequency stratospheric measurements could produce a statistically significant seasonal cycle to apply to β.

Acknowledgements. Support for this research was received from NASA's Carbon Cycle Science program (NNX10AT83G, James Randerson, PI). US funding for TCCON comes from NASA's Carbon Cycle Program, the Orbiting Carbon Observatory Program, and the DOE/ARM Program. European funding is from GEOMON, InGOS, and IMECC. Lauder measurements are supported by New Zealand Foundation of Research Science and Technology. Australian funding is from the Australian Research Council. Funding for the ACE-FTS mission is primarily provided by the Canadian Space Agency. SGP aircraft flask data were obtained through the ARM Program sponsored by the US Department of Energy, Office of Science, Office of Biological and Environmental Research and were generated by NOAA-ESRL, Carbon Cycle Greenhouse Gases Group. Baring Head NIWA surface data was provided courtesy of Gordon Brailsford, Dave Lowe and Ross Martin.

AMTD
7, 3471–3501, 2014

References

Angelbratt, J., Mellqvist, J., Blumenstock, T., Borsdorff, T., Brohede, S., Duchatelet, P., Forster, F., Hase, F., Mahieu, E., Murtagh, D., Petersen, A. K., Schneider, M., Sussmann, R., and Urban, J.: A new method to detect long term trends of methane (CH_4) and nitrous oxide (N_2O) total columns measured within the NDACC ground-based high resolution solar FTIR network, Atmos. Chem. Phys., 11, 6167–6183, doi:10.5194/acp-11-6167-2011, 2011. 3474

Bernath, P. F.: Atmospheric Chemistry Experiment (ACE): mission overview, Geophys. Res. Lett., 32, L15S01, doi:10.1029/2005GL022386, 2005. 3478

Connor, B. J., Boesch, H., Toon, G., Sen, B., Miller, C., and Crisp, D.: Orbiting carbon observatory: inverse method and prospective error analysis, J. Geophys. Res., 113, 1–14, doi:10.1029/2006JD008336, 2008. 3477, 3480

Dlugokencky, E. J.: Conversion of NOAA atmospheric dry air CH_4 mole fractions to a gravimetrically prepared standard scale, J. Geophys. Res., 110, D18306, doi:10.1029/2005JD006035, 2005. 3482

Keppel-Aleks, G., Wennberg, P. O., and Schneider, T.: Sources of variations in total column carbon dioxide, Atmos. Chem. Phys., 11, 3581–3593, doi:10.5194/acp-11-3581-2011, 2011. 3474

Lowe, D. C., Brenninkmeijer, C. A. M., Tyler, S. C., and Dlugkencky, E. J.: Determination of the isotopic composition of atmospheric methane and its application in the Antarctic, J. Geophys. Res., 96, 15455, doi:10.1029/91JD01119, 1991. 3483

Luo, M., Cicerone, R. J., Russell III, J. M., and Huang, T. Y. W.: Observations of stratospheric hydrogen fluoride by halogen occultation experiment (HALOE), J. Geophys. Res., 99, 16691–16705, 1994. 3475

Luo, M., Cicerone, R. J., and Russell III, J. M.: Analysis of halogen occultation experiment HF versus CH_4 correlation plots: chemistry and transport implications, J. Geophys. Res., 100, 13927–13937, 1995. 3475, 3478

Payne, V. H., Clough, S. A., Shephard, M. W., Nassar, R., and Logan, J. A.: Information-centered representation of retrievals with limited degrees of freedom for signal: application to methane from the tropospheric emission spectrometer, J. Geophys. Res., 114, D10307, doi:10.1029/2008JD010155, 2009. 3474

Rodgers, C. D. and Connor, B. J.: Intercomparison of remote sounding instruments, J. Geophys. Res., 108, 4116, doi:10.1029/2002JD002299, 2003. 3476

AMTD
7, 3471–3501, 2014

Sepúlveda, E., Schneider, M., Hase, F., García, O. E., Gomez-Pelaez, A., Dohe, S., Blumenstock, T., and Guerra, J. C.: Long-term validation of tropospheric column-averaged CH_4 mole fractions obtained by mid-infrared ground-based FTIR spectrometry, Atmos. Meas. Tech., 5, 1425–1441, doi:10.5194/amt-5-1425-2012, 2012. 3474

Sepúlveda, E., Schneider, M., Hase, F., Barthlott, S., Dubravica, D., García, O. E., Gomez-Pelaez, A., González, Y., Guerra, J. C., Gisi, M., Kohlhepp, R., Dohe, S., Blumenstock, T., Strong, K., Weaver, D., Palm, M., Sadeghi, A., Deutscher, N. M., Warneke, T., Notholt, J., Jones, N., Griffith, D. W. T., Smale, D., Brailsford, G. W., Robinson, J., Meinhardt, F., Steinbacher, M., Aalto, T., and Worthy, D.: Tropospheric CH_4 signals as observed by NDACC FTIR at globally distributed sites and comparison to GAW surface in-situ measurements, Atmos. Meas. Tech. Discuss., 7, 633–701, doi:10.5194/amtd-7-633-2014, 2014. 3474

Wang, Z., Deutscher, N. M., Warneke, T., Notholt, J., Dils, B., Griffith, D. W. T., Schmidt, M., Ramonet, M., and Gerbig, C.: Retrieval of tropospheric column-averaged CH_4 mole fraction by solar absorption FTIR-spectrometry using N_2O as a proxy, Atmos. Meas. Tech. Discuss., 7, 1457–1493, doi:10.5194/amtd-7-1457-2014, 2014. 3474

Washenfelder, R. A., Wennberg, P. O., and Toon, G. C.: Tropospheric methane retrieved from ground-based near-IR solar absorption spectra, Geophys. Res. Lett., 30, 2226, doi:10.1029/2003GL017969, 2003. 3474, 3475, 3478, 3481, 3492, 3498

Wunch, D., Toon, G. C., Wennberg, P. O., Wofsy, S. C., Stephens, B. B., Fischer, M. L., Uchino, O., Abshire, J. B., Bernath, P., Biraud, S. C., Blavier, J.-F. L., Boone, C., Bowman, K. P., Browell, E. V., Campos, T., Connor, B. J., Daube, B. C., Deutscher, N. M., Diao, M., Elkins, J. W., Gerbig, C., Gottlieb, E., Griffith, D. W. T., Hurst, D. F., Jiménez, R., Keppel-Aleks, G., Kort, E. A., Macatangay, R., Machida, T., Matsueda, H., Moore, F., Morino, I., Park, S., Robinson, J., Roehl, C. M., Sawa, Y., Sherlock, V., Sweeney, C., Tanaka, T., and Zondlo, M. A.: Calibration of the Total Carbon Column Observing Network using aircraft profile data, Atmos. Meas. Tech., 3, 1351–1362, doi:10.5194/amt-3-1351-2010, 2010. 3476, 3482

Wunch, D., Toon, G. C., Blavier, J.-F. L., Washenfelder, R. A., Notholt, J., Connor, B. J., Griffith, D. W. T., Sherlock, V., and Wennberg, P. O.: The Total Carbon Column Observing Network, Philos. T. R. Soc. A, 369, 2087–2112, doi:10.1098/rsta.2010.0240, 2011a. 3474, 3476

Wunch, D., Wennberg, P. O., Toon, G. C., Connor, B. J., Fisher, B., Osterman, G. B., Frankenberg, C., Mandrake, L., O'Dell, C., Ahonen, P., Biraud, S. C., Castano, R., Cressie, N., Crisp, D., Deutscher, N. M., Eldering, A., Fisher, M. L., Griffith, D. W. T., Gunson, M., Heikki-

AMTD
7, 3471–3501, 2014

nen, P., Keppel-Aleks, G., Kyrö, E., Lindenmaier, R., Macatangay, R., Mendonca, J., Messerschmidt, J., Miller, C. E., Morino, I., Notholt, J., Oyafuso, F. A., Rettinger, M., Robinson, J., Roehl, C. M., Salawitch, R. J., Sherlock, V., Strong, K., Sussmann, R., Tanaka, T., Thompson, D. R., Uchino, O., Warneke, T., and Wofsy, S. C.: A method for evaluating bias in global measurements of CO_2 total columns from space, Atmos. Chem. Phys., 11, 12317–12337, doi:10.5194/acp-11-12317-2011, 2011b. 3477, 3480

Yang, Z., Washenfelder, R. A., Keppel-Aleks, G., Krakauer, N. Y., Randerson, J. T., Tans, P. P., Sweeney, C., and Wennberg, P. O.: New constraints on Northern Hemisphere growing season net flux, Geophys. Res. Lett., 34, L12807, doi:10.1029/2007GL029742, 2007. 3474

York, D., Evensen, N. M., Martínez, M. L., and De Basabe Delgado, J.: Unified equations for the slope, intercept, and standard errors of the best straight line, Am. J. Phys., 72, 367, doi:10.1119/1.1632486, 2004. 3482

AMTD
7, 3471–3501, 2014

Table 1. Zonal and annual values (2σ errors) of β.

	60–90° S	30–60° S	0–30° S	0–30° N	30–60° N	60–90° N
2004	−719 (7)	−706 (10)	−674 (28)	−714 (17)	−739 (7)	−756 (5)
2005	−739 (5)	−729 (7)	−701 (18)	−633 (22)	−740 (6)	−748 (4)
2006	−742 (6)	−725 (9)	−648 (25)	−690 (18)	−752 (7)	−758 (5)
2007	−738 (6)	−730 (9)	−684 (31)	−620 (50)	−742 (8)	−754 (5)
2008	−743 (6)	−732 (8)	−665 (25)	−705 (23)	−734 (6)	−749 (4)
2009	−727 (6)	−721 (10)	−635 (36)	−661 (28)	−743 (9)	−755 (6)
2010	−706 (5)	−709 (7)	−658 (22)	−656 (27)	−716 (7)	−737 (4)
2011	−746 (5)	−735 (9)	−596 (61)	−607 (25)	−704 (6)	−731 (4)
2012	−714 (7)	−705 (8)	−624 (51)	−641 (24)	−722 (7)	−724 (5)
2013	−712 (23)	−703 (20)	−622 (63)	−639 (63)	−720 (16)	−722 (11)

AMTD
7, 3471–3501, 2014

Table 2. TCCON sites, coordinates, altitudes, and locations.

Site	Latitude	Longitude	Elevation (km)	Location
Sodankylä	67.4	26.6	0.18	Sodankylä, Finland
Bremen	53.1	8.85	0.03	Bremen, Germany
Park Falls	45.9	−90.3	0.44	Park Falls, WI
Lamont	36.6	−97.5	0.32	Lamont, OK
Izaña	28.3	−16.5	2.37	Tenerife, Canary Islands
Darwin	−12.4	130.9	0.03	Darwin, Australia
Wollongong	−34.4	150.9	0.03	Wollongong, Australia
Lauder	−45.0	169.7	0.37	Lauder, NZ

AMTD
7, 3471–3501, 2014

Table 3. Aircraft Overflights. TCCON site locations and aircraft campaign dates and altitude ranges are listed.

Site	Location	Campaign	Date	Altitude Range
Park Falls	46° N, 90° W	INTEX	12 Jul 2004	0.7–10.1 km
		START08	12 May 2008	1.2–9.4 km
Lamont	37° N, 98° W	HIPPO	30 Jan 2009	0.4–13.0 km
		Learjet	31 Jul; 2, 3 Aug 2009	0.5–12.9 km
Wollongong	34° S, 151° E	HIPPO	15 Nov 2009	0.1–12.6 km
Lauder	45° S, 170° E	HIPPO	20 Jan 2009	0.7–14.6 km

AMTD
7, 3471–3501, 2014

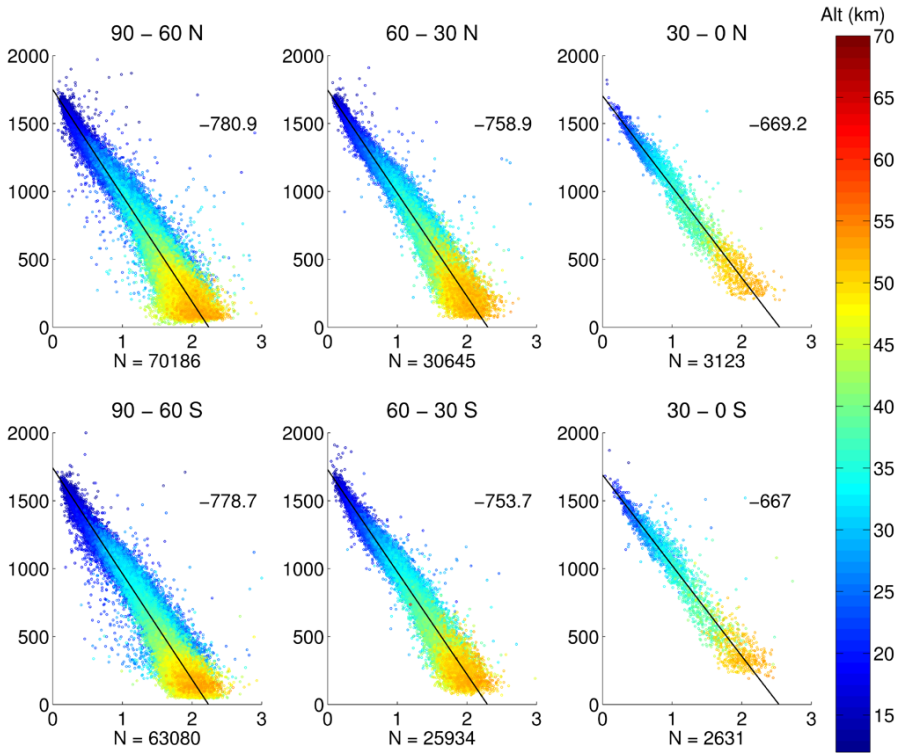

Fig. 1. CH_4 (ppb, *y* axis) vs. HF (ppb, *x* axis) from ACE-FTS, binned by latitude bands. Plot titles correspond to the upper zonal extent. The slopes (β) are in the upper right-hand corner, and number of data points (*N*) are listed below each plot.

AMTD
7, 3471–3501, 2014

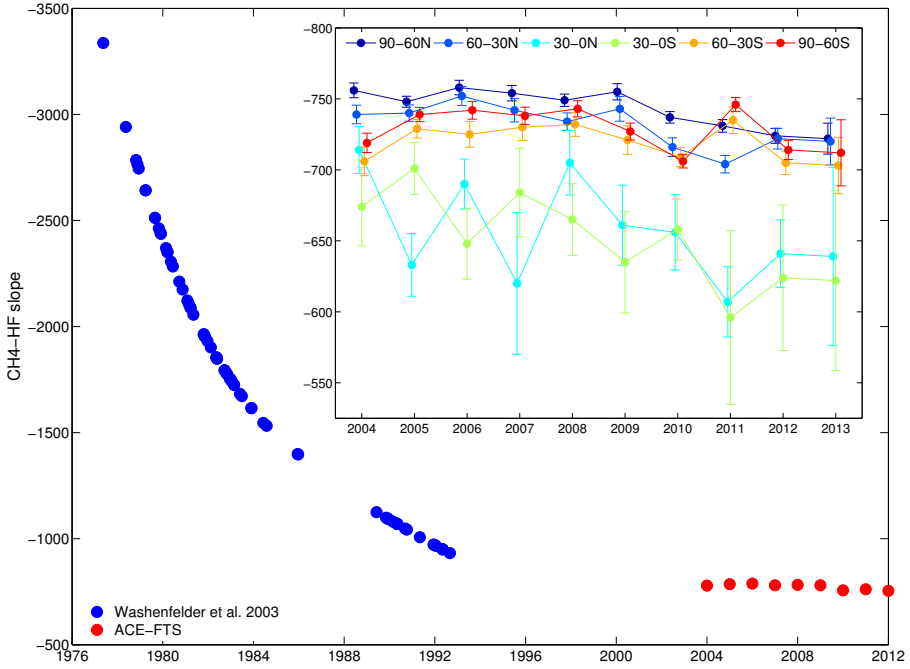

Fig. 2. Long-term CH_4–HF slopes derived by Washenfelder et al. (2003) and annual-mean slopes from ACE-FTS. The inset shows the zonal ACE-FTS slopes for each year, with error bars denoting the 2σ standard error. For each year, zonal slopes are offset from each other for clarity.

AMTD
7, 3471–3501, 2014

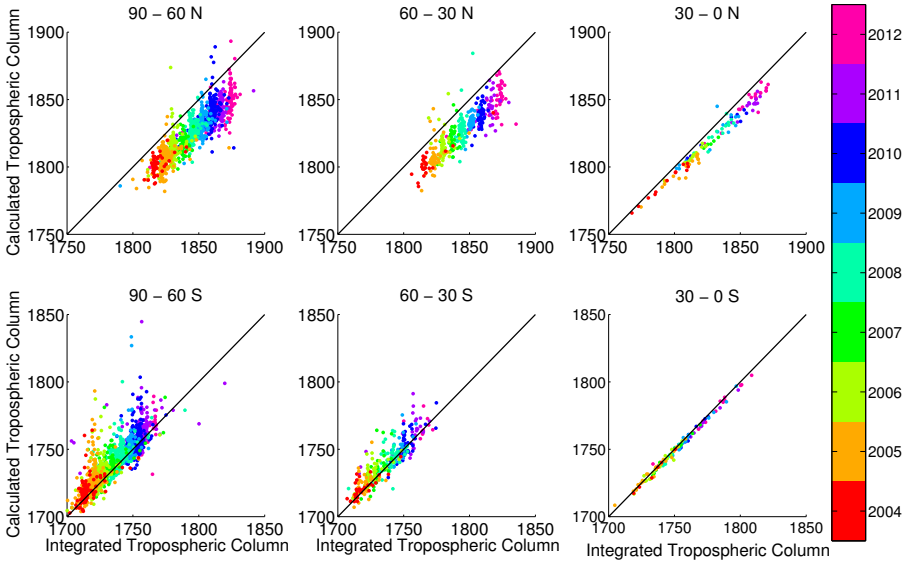

Fig. 3. Validation of the tropospheric column averaged CH_4 derivation using HF as a proxy. The calculated tropospheric CH_4 (y axis) uses the TCCON priors and CH_4 averaging kernel and ACE-FTS vertical profiles to determine the value that the ground-based FTS would retrieve. The integrated tropospheric CH_4 (x axis) applies the pressure-weighting function and TCCON CH_4 averaging kernel and priors to the extrapolated tropospheric ACE-FTS profile of CH_4. Note the different DMF ranges in the Northern vs. Southern Hemispheres.

AMTD
7, 3471–3501, 2014

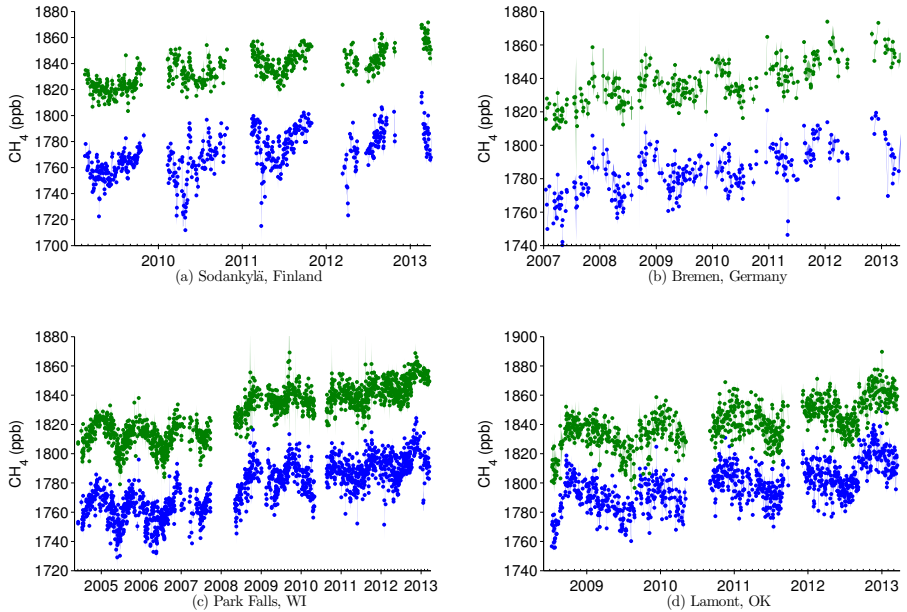

Fig. 4. Daily median and standard deviation (shading) total (blue) and tropospheric (green) column-averaged DMFs of CH_4 at **(a)** Sodankylä, Finland, **(b)** Bremen, Germany, **(c)** Park Falls, Wisconsin, USA, and **(d)** Lamont, Oklahoma, USA. Only days with more than 5 measurements of tropospheric CH_4 with errors of < 1 % are included.

AMTD
7, 3471–3501, 2014

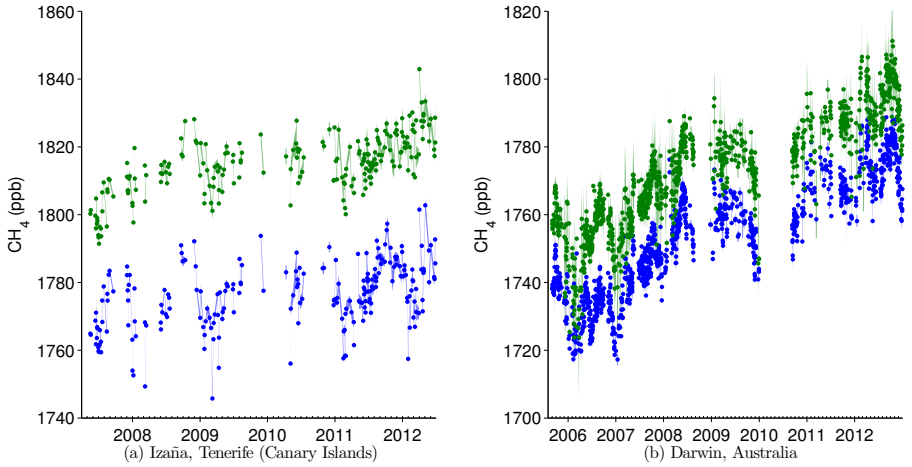

Fig. 5. Same as Fig. 4 for **(a)** Izaña, Tenerife, Canary Islands and **(b)** Darwin, Australia.

AMTD
7, 3471–3501, 2014

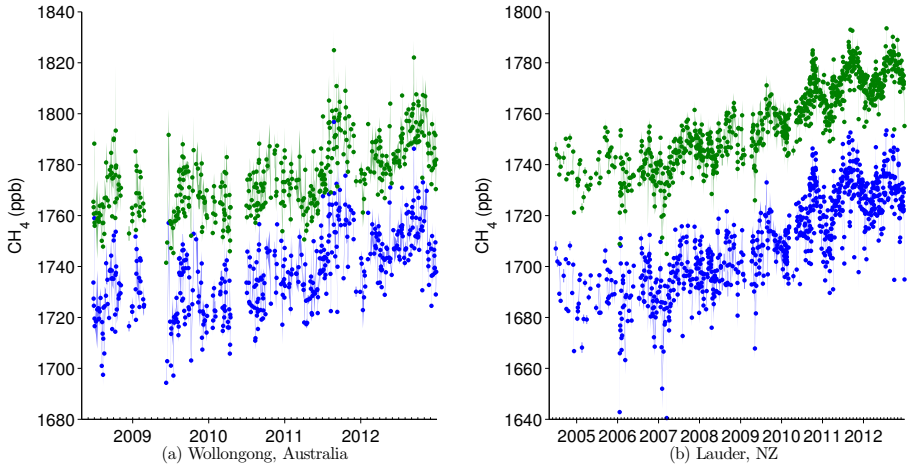

Fig. 6. Same as Fig. 4 for **(a)** Wollongong, Australia and **(b)** Lauder, New Zealand. Both the 120 HR (June 2004–December 2010) and 125 HR (February 2010–December 2012) instruments are plotted for Lauder.

AMTD
7, 3471–3501, 2014

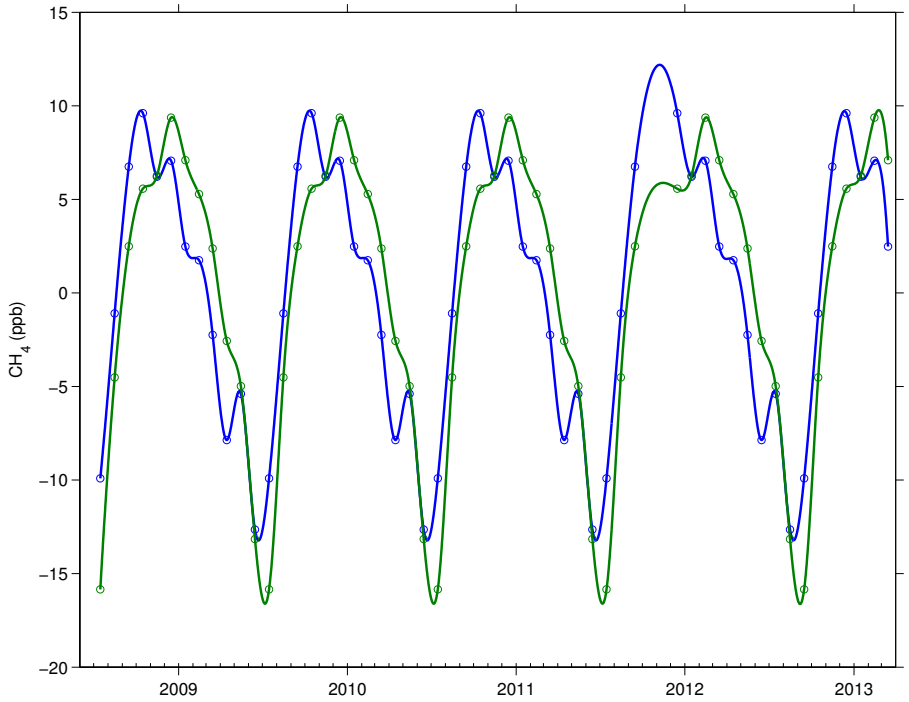

Fig. 7. Detrended seasonal cycles of CH_4 at Lamont for total columns (blue) and tropospheric columns (green).

AMTD
7, 3471–3501, 2014

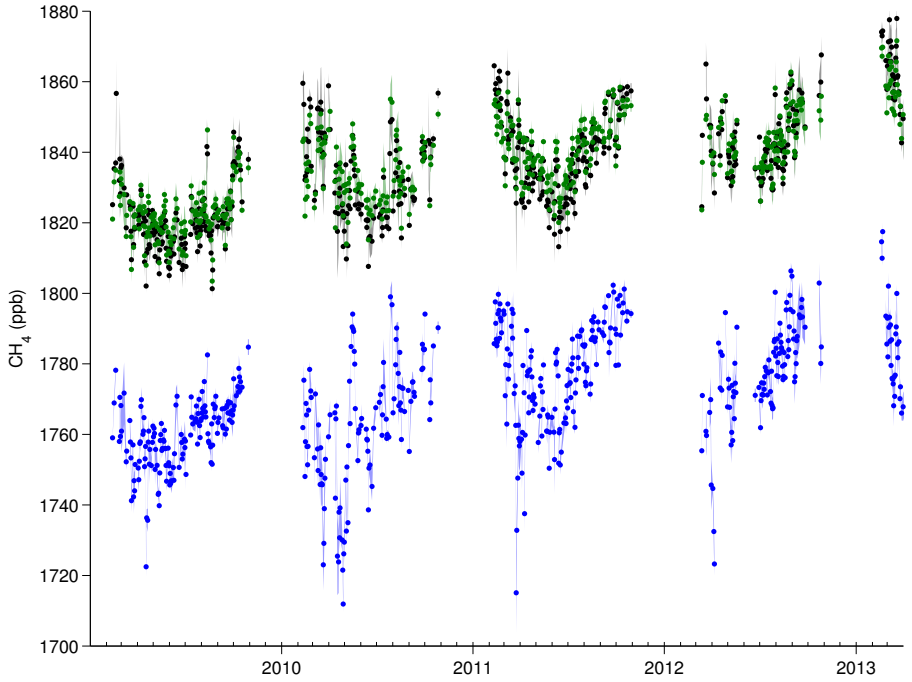

Fig. 8. Daily median total and tropospheric column-averaged DMFs at Sodankylä using the Washenfelder et al. (2003) method (black) vs. the updated method (green). Tropospheric and total columns DMFs are the same as in Fig. 4.

AMTD
7, 3471–3501, 2014

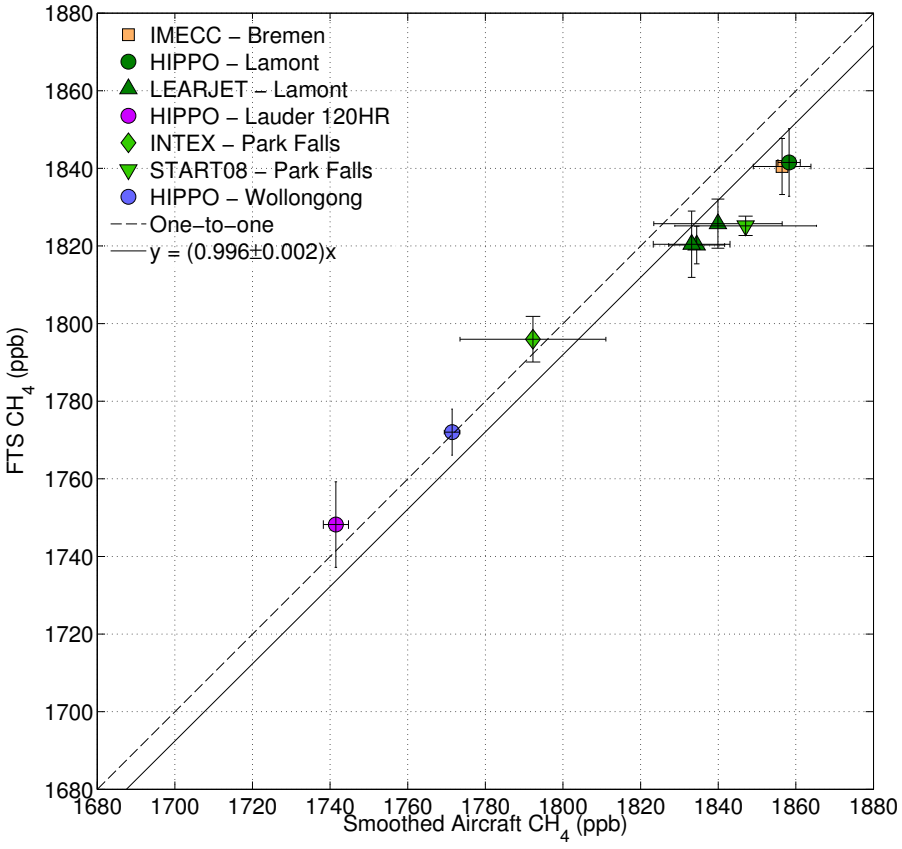

Fig. 9. Tropospheric CH_4 column comparison for TCCON vs. aircraft profiles. Error bars denote the 2σ standard deviation from the median (FTS) and the estimated instrument errors and tropospheric uncertainty of the measurements (aircraft).

AMTD
7, 3471–3501, 2014

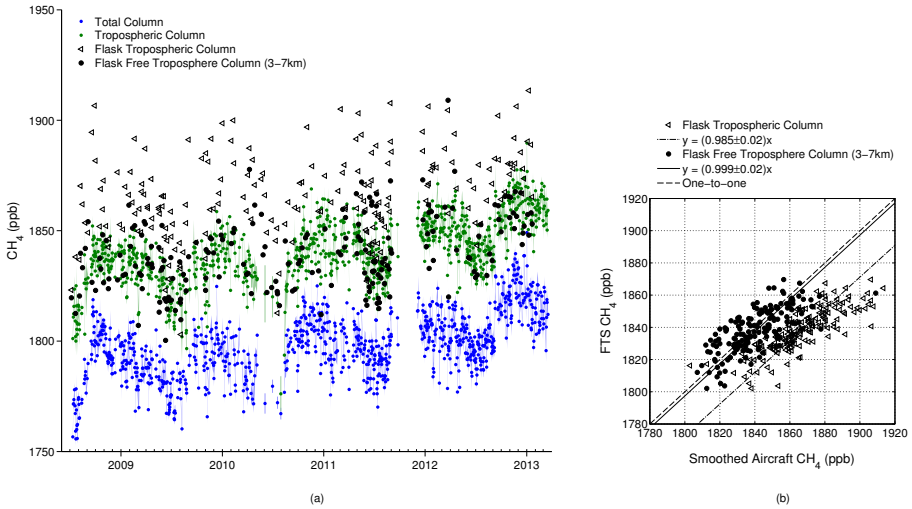

Fig. 10. (a) Daily median column and aircraft CH_4 DMFs at Lamont. Only days with more than 5 measurements of FTS-derived tropospheric CH_4 with errors of < 1 % are included. **(b)** Tropospheric CH_4 column comparison for TCCON vs. in situ profiles.

AMTD
7, 3471–3501, 2014

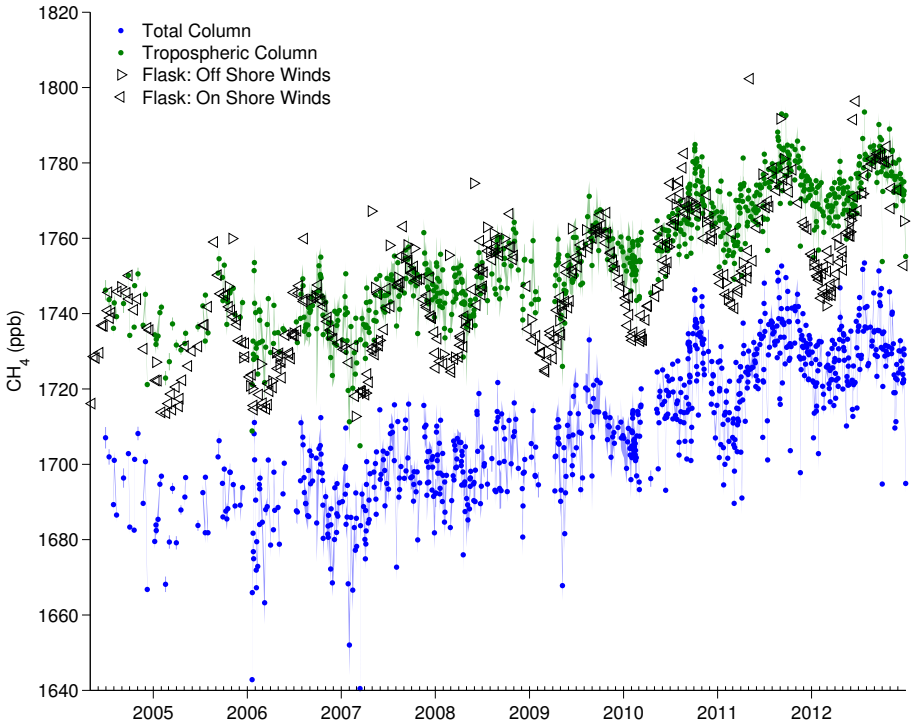

Fig. 11. Daily median CH_4 DMFs at Lauder (FTS) and Baring Head (flask). Both the 120 HR (June 2004–December 2010) and 125 HR (February 2010–December 2012) instruments are plotted for Lauder. Only days with more than 5 measurements of FTS-derived tropospheric CH_4 with errors of < 1 % are included.

AMTD
7, 3471–3501, 2014